Supplementary Material for

A BAK Subdomain That Binds Mitochondrial Lipids Selectively and Releases Cytochrome C

Haiming Dai, Kevin L. Peterson, Karen S. Flatten, X. Wei Meng, Annapoorna Venkatachalam, Cristina Correia, Marina Ramirez-Alvarado, Yuan-Ping Pang, and Scott H. Kaufmann

SUPPLEMENTARY RESULTS AND DISCUSSION

Conformational analysis of tandem peptides and their variants

Molecular dynamics simulations with an aggregated time of 37.92 μs were performed for α4-α5, α5-α6 and α6-α7/8 and several of their variants to probe their conformational characteristics. **Table S1**, which contains information on the top three most populated conformations for each peptide, indicates that the most populated or second most populated conformation of peptides α4-α5, α5-α5, α5-α6, and α6-α7/8 had two U-shaped helices, whereas all variants except for the sequence of α6-α7/8Δ12 did not adopt the U-shaped conformation (**Figs. 3 and S5**). Interestingly, each U-shaped conformation had the maximal interhelical hydrophobic, pi-pi, or aromatic interactions as revealed by the sphere models in **Fig. 3**. Notably, the U-shaped conformation of α6-α7/8 had the cationic Arg residue stabilized by a cluster of five aromatic residues, potentially allowing α6-α7/8 to interact more favorably with the anionic membrane than other U-shaped peptides even though the population of the U-shaped α6-α7/8 conformation was smaller than those of other U-shaped peptides (**Table S1**). The U-shaped α6-α7/8Δ12 conformation also had the cationic Arg residue stabilized by a Trp side chain, but this shortened peptide failed to cause MOMP (**Fig. S13**). These results suggest that the common characteristics of the tandem peptides that are able to induce MOMP might be two long helices in a U shaped conformation with substantial interhelical interactions.

BAK protein conformations with protruding U-shaped tandem peptides

A recent x-ray crystallography study has reported a structure of detergent-activated BAK in which α6-α7/8 is in the conformation of a single long helix (ref. 22). The molecular dynamics simulations summarized in **Table S1**, however, predict that an alternative conformation consisting of two long helices in a U-shaped conformation is almost as frequently populated as the single long linear conformation. In view of the biological effects of the α4-α5, α5-α6, and α6-α7/8 tandem peptides, which include lipid binding (**Fig. 5**), localization of bound proteins to mitochondria (**Fig. 2**), and permeabilization of the MOM (**Fig. 4**) *in vitro* and *in vivo*, we assessed the ability of BAK to protrude, without severe steric clashes that cause stereochemical violations, one of the tandem peptides in a U-shaped conformation with two helices long enough to span the MOM. Because protein folding and complexation pathways are often heterogeneous and cooperative [1, 2], we also examined the possibility that more than one of these tandem peptides could be protruded. Subsequent modeling of the BAK crystal structure led to the backbone conformations of BAK shown in **Fig. 8F** and **Fig. S16**, which suggest that BAK could structurally protrude, without steric clashes that cause any epimerization or isomerization, one or more of the α4-α5, α5-α6, and α6-α7/8 sequences in a conformation with two helices in a U-shaped conformation.

SUPPLEMENTARY METHODS

Circular Dichroism (CD) Spectroscopy. Far UV CD spectra of the different peptides were acquired in the CD spectropolarimeter (JASCO 810) at room temperature with a 0.1 cm path-length quartz cuvette as previously reported [3].

Conformational analyses of tandem peptides and their variants. The initial conformations of α4-α5 and α5-α6 were taken from the BAK crystal structure (Protein Data Bank ID: 2IMS). The initial conformation α6-α7/8 was manually mutated from the α5-α6 conformation. The initial conformations of 12 variants of these peptides (Supplementary Table S1) were manually mutated from respective parent peptides. The resulting initial conformations were each refined with energy minimization followed by 20 1.896-μs molecular dynamics (MD) simulations using FF12MC [4]. All peptide topology and coordinate files were generated by tLEaP of the AmberTools 20 package (University of California, San Francisco). The forcefield parameter file of FF12MC and the tLEaP input file for loading FF12MC and the Cartesian coordinates of all 15 energy-minimized peptide conformations as the initial conformations for MD simulations are provided in Data S1 and S2, respectively. The energy minimization and MD simulations of each peptide were performed respectively using SANDER of AMBER 20 and PMEMD of AMBER 18/20 (University of California, San Francisco) and FF12MC. The energy minimization used dielectric constant of 1.0 and 100 cycles of steepest-descent minimization followed by 900 cycles of conjugate-gradient minimization. The energy-minimized peptide conformation was neutralized with sodium or chloride and then solvated with TIP3P water molecules [5] and energy-minimized for 100 cycles as above followed by 900 cycles of conjugate-gradient minimization to remove close van der Waals contacts. The resulting system was then heated to 340 K in 30 steps under constant temperature and volume, equilibrated for 10^6 timesteps under constant temperature of 340 K and constant pressure of 1 atm employing isotropic molecule-based scaling, and finally simulated in 20 distinct, independent, unrestricted, unbiased, and classical isobaric–isothermal MD simulations using a periodic boundary condition at 340 K and 1 atm with isotropic molecule-based scaling. The use of 340 K in the simulations was for better conformational sampling, according to the reports that protein folding times derived from the MD simulations employing FF12MC are inversely related to simulation temperatures and in excellent agreement with experimentally determined folding times at different temperatures [4, 6]. All simulations used (i) a dielectric constant of 1.0, (ii) the Berendsen coupling algorithm [7] for thermostat and barostat, (iii) the Particle Mesh Ewald method [8] to calculate electrostatic interactions of two atoms at a separation of >8 Å, (iv) Δt = 1.00 fs of the standard-mass time [4, 9], (v) the SHAKE-bond-length constraint applied to all the bonds involving hydrogen, (vi) a protocol to save the image closest to the middle of the "primary box" to the restart and trajectory files, (vii) a formatted restart file, (viii) the revised sodium and chloride parameters [10], (ix) a cutoff of 8.0 Å for noncovalent interactions, (x) a uniform 10-fold reduction in the atomic masses of the entire simulation system (both solute and solvent) [4, 9], (xi) NTWX = 200,000 steps for coordinate output, and (xii) default values of all other inputs of PMEMD. All simulations were performed on computers at the University of Minnesota Supercomputing Institute (Minneapolis, MN) using PMEMD of AMBER 20 and the Mayo Clinic high-performance computing facility at the University of Illinois Urbana-Champaign National Center for Supercomputing Applications using PMEMD of AMBER 18. The

conformational cluster analysis of each peptide (using all 60,000 conformations from 20 1.896-μs MD simulations) was performed using the CPPTRAJ.MPI module of AmberTools 20 with the average-linkage algorithm [11] (epsilon = 4.0 Å; RMS on all CA atoms except those at the three terminal residues). The Cartesian coordinates of the top-three most populated conformations for each of the 15 peptides derived from the 20 1.896-μs MD simulations are provided in Data S3.

Cartoons of BAK Protein with tandem helices in membrane. The BAK protein conformations with protruding tandem helices shown in Fig. 8F and Supplementary Fig. S15 were obtained from the *apo*-BAK crystal structure (Protein Data Bank ID: 2IMS) through deleting the crystallographically determined α4-α5 or α6-α7/8 conformation followed by manually inserting the afore-described energy minimized α4-α5 or α6-α7/8 conformations in such a way that the tandem helices protrude without severe steric clashes. The resulting conformation of the BAK with protruding tandem helices was then energy minimized using the protocol described above and quality checked using the PROCHECK program [12] to ensure without any stereochemical violations.

SUPPLEMENTARY REFERENCES

1. Fersht AR. On the simulation of protein folding by short time scale molecular dynamics and distributed computing. *Proc Natl Acad Sci U S A* 2002; **99**: 14122-14125.
2. Pang Y-P. How neocarcerand Octacid4 self-assembles with guests into irreversible noncovalent complexes and what accelerates the assembly. *Communications Chemistry* 2022; **5**: 9.
3. Dai H, Pang Y-P, Ramirez-Alvarado M, Kaufmann SH. Evaluation of the BH3-Only Protein Puma as a Direct Bak Activator. *J Biol Chem* 2014; **289**: 89-99.
4. Pang YP. FF12MC: A revised AMBER forcefield and new protein simulation protocol. *Proteins* 2016; **84**: 1490-1516.
5. Jorgensen WL, Chandreskhar J, Madura JD, Impey RW, Klein ML. Comparison of simple potential functions for simulating liquid water. *J Chem Phys* 1983; **79**: 926–935.
6. Pang YP. How fast fast-folding proteins fold in silico. *Biochem Biophys Res Commun* 2017; **492**: 135-139.
7. Berendsen HJC, Postma JPM, van Gunsteren WF, Di Nola A, Haak JR. Molecular dynamics with coupling to an external bath. *J Chem Phys* 1984; **81**: 3684–3690.
8. Darden TA, York DM, Pedersen LG. Particle mesh Ewald: An N log(N) method for Ewald sums in large systems. *J Chem Phys* 1993; **98**: 10089–10092.
9. Pang YP. Low-mass molecular dynamics simulation for configurational sampling enhancement: More evidence and theoretical explanation. *Biochem Biophys Rep* 2015; **4**: 126-133.
10. Joung IS, Cheatham TE. Determination of alkali and halide monovalent ion parameters for use in explicitly solvated biomolecular simulations. *J Phys Chem B* 2008; **112**: 9020–9041.
11. Shao J, Tanner SW, Thompson N, Cheatham III TE. Clustering molecular dynamics trajectories: 1. Characterizing the performance of different clustering algorithms. *J Chem Theory Comput* 2007; **3**: 2312–2334.
12. Laskowski RA, MacArthur MW, Moss DS, Thornton JM. PROCHECK: a program to check the stereochemical quality of protein structures. *J Appl Cryst* 1993; **26**: 283–291.

Table S1

Conformational cluster analysis of molecular dynamics simulations of 15 peptides using 60,000 conformers for each peptide

Number of clusters	Number of conformers in each of the top 3 clusters	Occurrence of each cluster (%)	Structural details[a,b]	Average crystallographically determined backbone (N CA C O) B factors (Å^2)
			α4-α5 (Fig. 6)	
	15991	27	2 parallel helices (U-shaped; α:1-5 & 11-42; π:6-10)	
99	6889	12	3 helices	16 (from 2IMS); 20 (from 2IMT)
	4067	7	3 helices	
			α4-α5 3E (Fig. 6)	
	11616	19	2 slightly orthogonal helices	
269	3061	5	2 slightly orthogonal helices	not available
	2812	5	3 helices	
			α5-α5 (Fig. 7)	
	9062	15	3 helices	
99	8183	14	2 parallel helices (U-shaped)	not available
	8057	13	2 slightly orthogonal helices	
			α5-α6 (Fig. 6)	
	14817	25	2 nearly orthogonal helices	
71	9632	16	2 parallel helices (U-shaped; α:11-23 and 26-34; π:1-10)	14 (from 2IMS); 19 (from 2IMT)
	4950	8	3 helices	
			α5-α6 3E (Fig. 6)	
	8915	15	2 nearly orthogonal helices	
199	5303	9	3 helices	not available
	5157	9	2 orthogonal helices	
			α5-α9 (Fig. 7)	
	4202	7	2 nearly orthogonal helices	
155	4142	7	3 helices	not available
	2972	5	3 helices	
			α6-α7/8 (Fig. 6)	
	4111	7	1 long helix (α:1-9; π:10-38)	
474	3376	6	2 parallel helices (U-shaped)	17 (from 2IMS); 23 (from 2IMT)
	3239	5	3 helices	
			α6-α7/8 3E (Fig. 6)	
	9794	16	2 slightly orthogonal helices	
466	5274	9	3 helices	not available
	2483	4	1 long helix (α:1-9; π:10-26) and 1 short helix (α:28-35)	
			α4-α5 2P (Fig. 7)	
	12578	21	2 nearly orthogonal helices	
94	7633	13	2 slightly orthogonal helices	not available
	3707	6	3 helices	
			α5-α6 4P (Fig. 7)	
	6454	11	2 orthogonal short helices	
274	5259	9	2 nearly orthogonal helices	not available
	3919	7	2 orthogonal helices	

			α6-α7/8 4P (Fig. 7)	
	11312	19	2 nearly orthogonal helices	
527	4707	8	3 helices	not available
	2996	5	2 nearly orthogonal short helices	
			α5-α6 Δ6 (Fig. 8)	
	15914	27	2 nearly orthogonal helices	
195	13802	23	2 nearly orthogonal helices	not available
	3624	6	3 helices	
			α5-α6 Δ12 (Fig. 8)	
	13842	23	1 helix	
315	12601	21	2 short, slightly orthogonal helices	not available
	6797	11	2 short, slightly orthogonal helices	
			α6-α7/8 Δ6 (Fig. S15)	
	2213	4	3 helices	
842	1712	3	2 parallel helices (one long and one short)	not available
	1553	3	3 helices	
			α6-α7/8 Δ12 (Fig. S15)	
	5298	11	2 short parallel helices (U-shaped)	
768	5040	10	2 short parallel helices (U-shaped)	not available
	3653	7	2 parallel β-strands (hairpin)	

[a]Structures of the top two conformations are shown in **Fig. 3** and the top three conformations are shown in **Fig. S5**.

[b]Figure numbers indicate figures where the amino acid sequences of the wildtype and variant peptides are shown.

SUPPLEMENTARY FIGURES

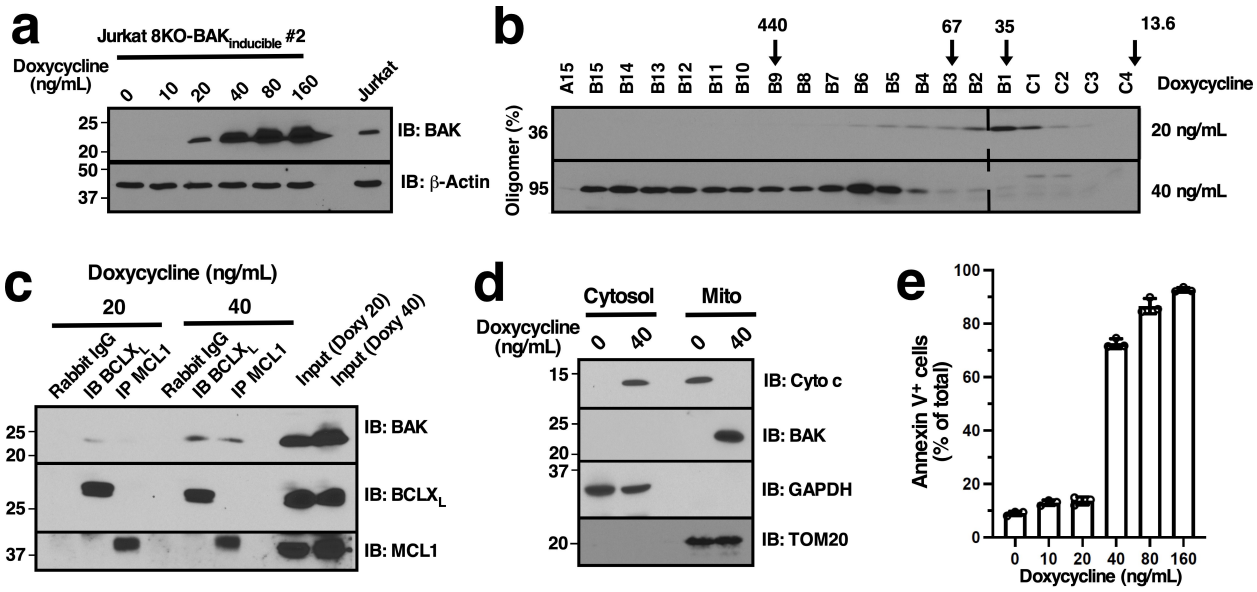

Figure S1. Concentration-dependent BAK activation in the absence of exogenous stimuli. Jurkat 8KO cells (lacking BAX, BAK, BID, BIM, PUMA, NOXA, BMF and HRK) were transduced with cDNA encoding BAK behind a doxycycline-inducible promoter. **a** Immunoblot showing BAK expression after treatment for 16 h with various doxycycline concentrations in the presence of Q-VD-OPh to prevent caspase-mediated events. **b** Size exclusion chromatography showing BAK oligomerization state after BAK induction to different levels. Purified monomeric BAKΔTM runs in fractions B1-C3 on this column (ref. 8 in main text).The percentage of BAK in oligomers was calculated as described in ref. 36 of the main text. **c** After treatment of cells with the indicated concentrations of doxycycline for 16 h in the presence of Q-VD-OPh, cell lysates were subjected to immunoprecipitation with antibodies to $BCLX_L$ or MCL1 as previously described (ref. 36 in main text). Note the increased binding to $BCLX_L$ and MCL1, which is dependent on externalization of the BAK BH3 domain, at the higher doxycycline concentration. **d** After cells were treated with the indicated concentration of doxycycline along with Q-VD-OPh for 24 h, crude mitochondria (mito) and cytosol were isolated and subjected to immunoblotting. **e** Cells were treated with the indicated concentration of doxycycline in the absence of Q-VD-OPh for 24 h and stained with Annexin V.

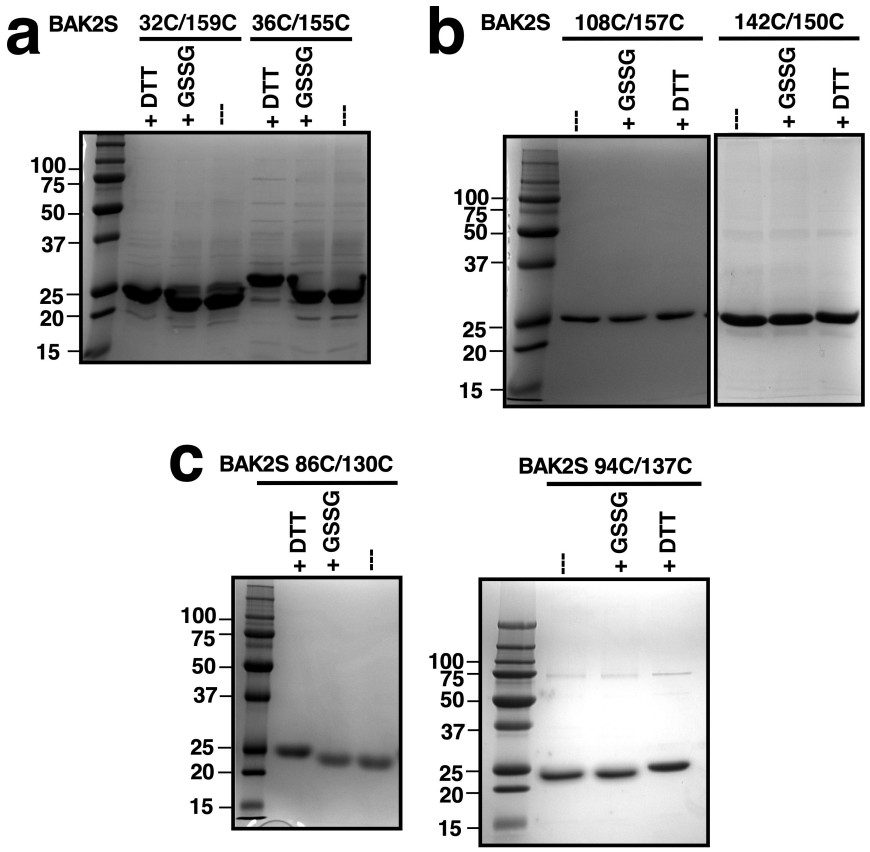

Figure S2 (related to Figure 1). Purified BAK2S/2C mutants used in this study are oxidized. After pre-treatment with buffer, 5 mM DTT or 5 mM oxidized GSH for 2 h at 20-22 °C, the indicated BAK 2S 32C/159C and 36C/155C mutants (a), 108C/157C and 142C/150C mutants (b), or 86C/130C and 94C/137C mutants (c) were separated by non-reducing SDS-PAGE and stained with Coomassie blue.

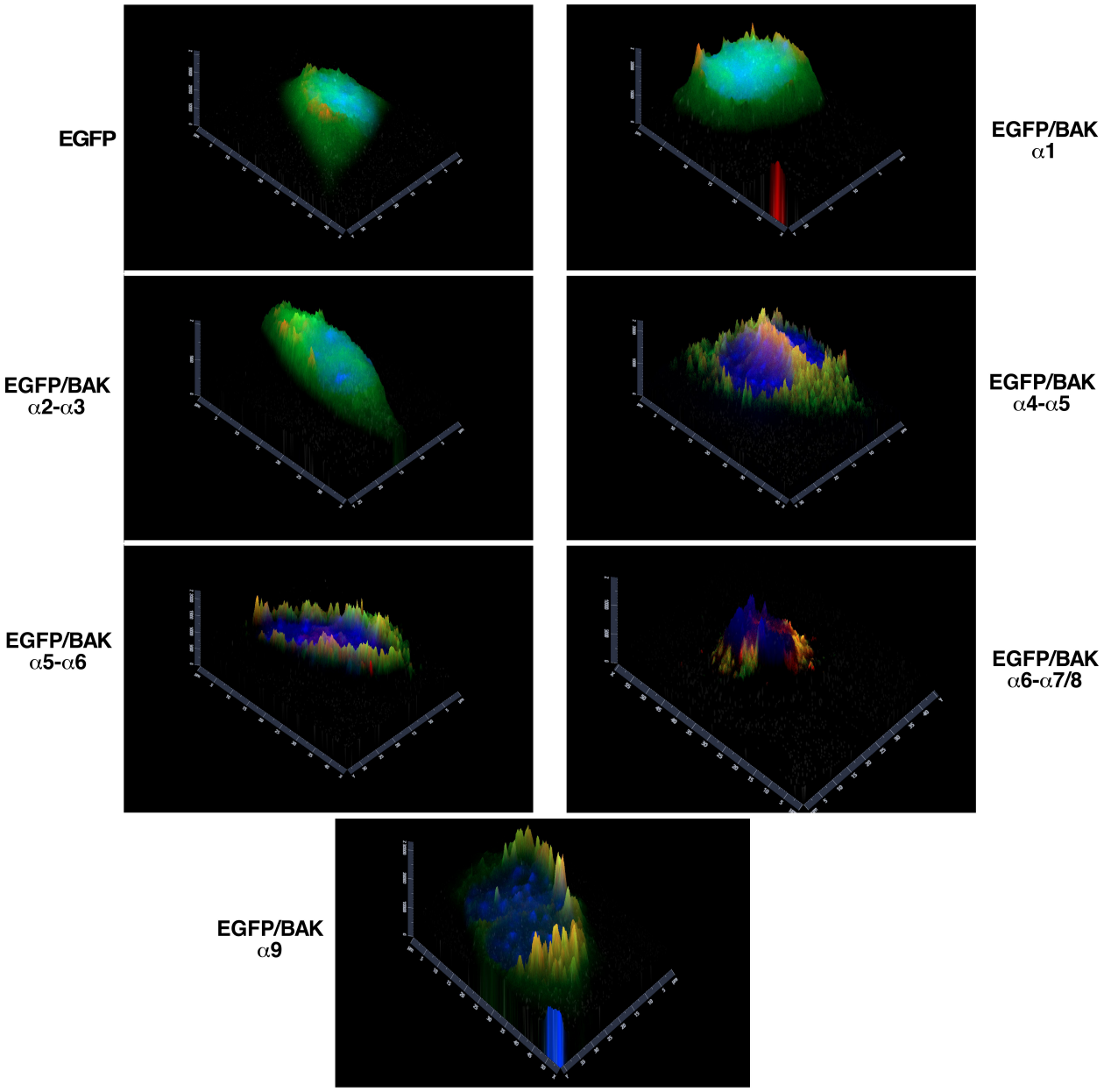

Figure S3 (related to Figure 2). Superimposed histograms of Mitotracker red, EGFP or EGFP-fusion proteins (green) and Hoechst 3358 (blue) intensities. Panels shown in Figure 2 were examined on a pixel-by-pixel basis using Zeiss Zen software. Yellow indicates co-localization of red and green signals.

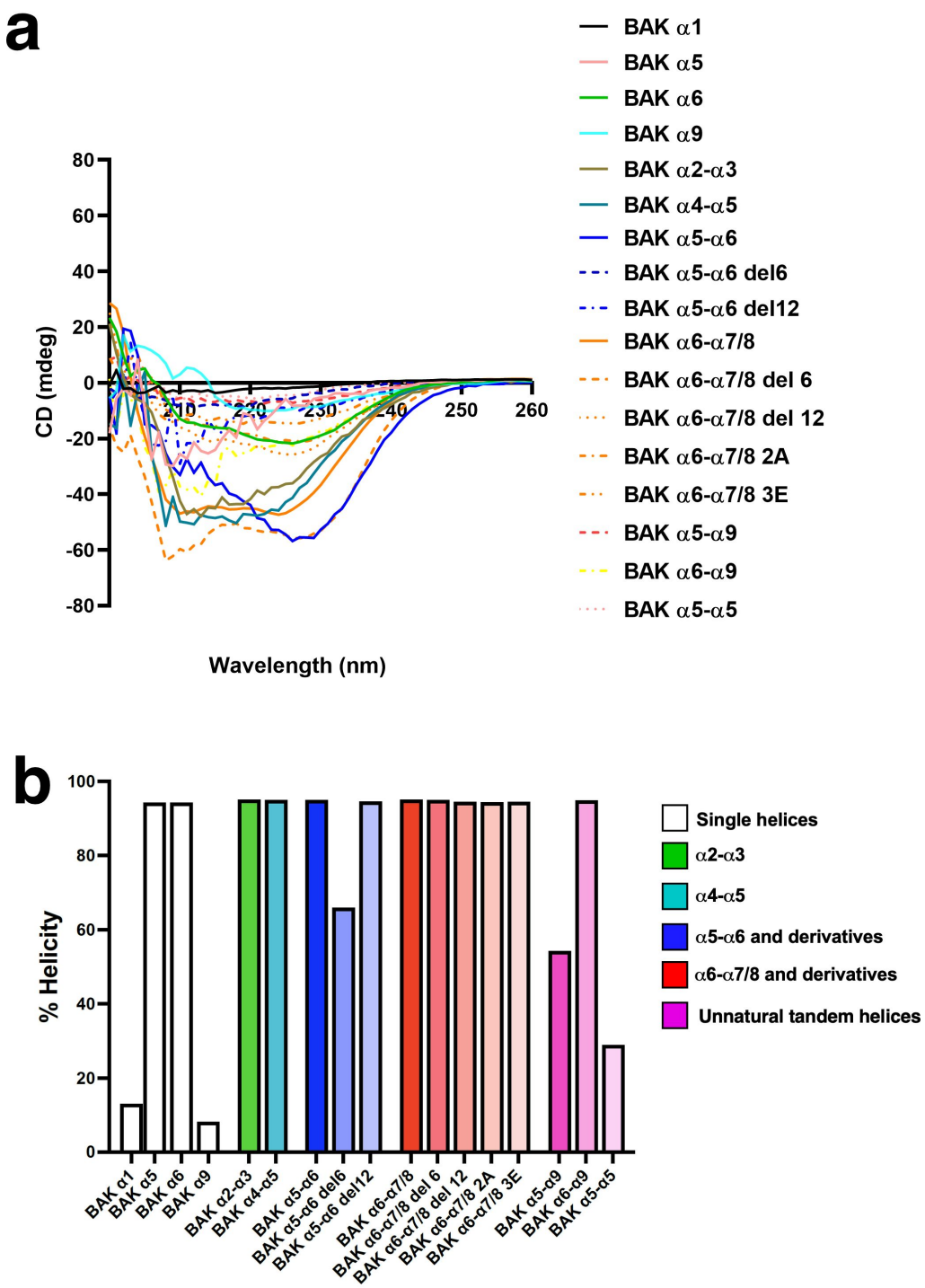

Figure S4 (related to Figure 3). Circular dichroism (CD) spectra of peptides used in this study. a Far UV-CD spectra of peptides (0.2 mg/mL) were measured in HK buffer. **b** Helical content of the peptides calculated using the data from CD experiments.

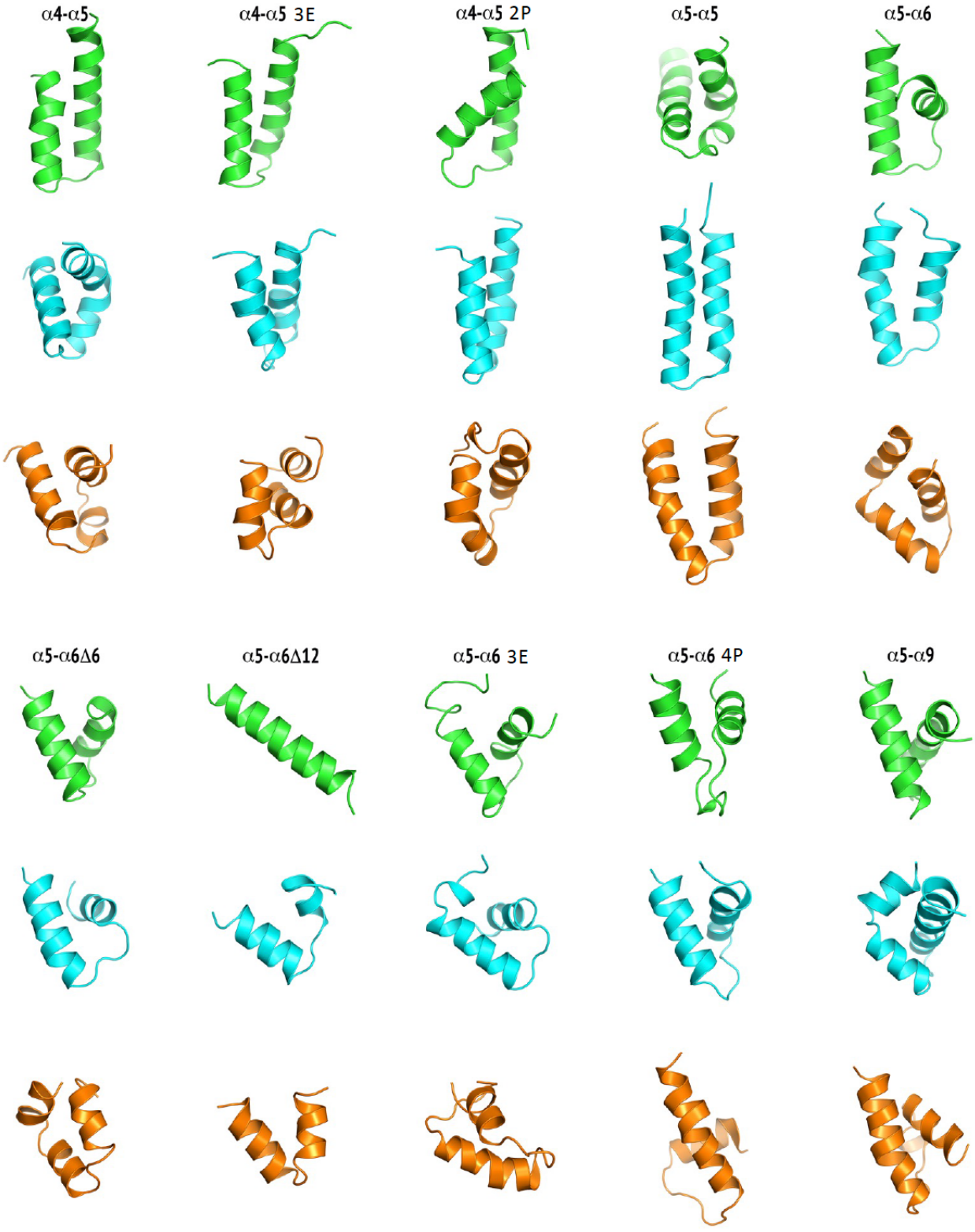
α4-α5
α4-α5 3E
α4-α5 2P
α5-α5
α5-α6
α5-α6Δ6
α5-α6Δ12
α5-α6 3E
α5-α6 4P
α5-α9

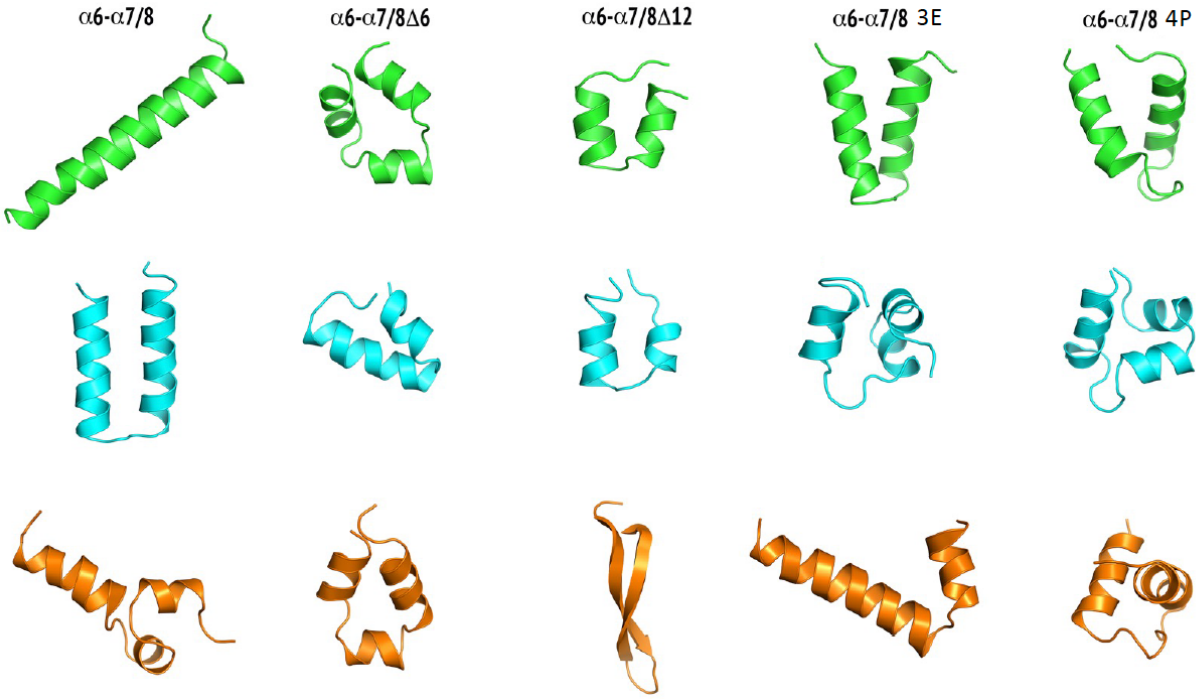

Figure S5 (Related to Figure 3 and Table S1). The top three most populated backbone conformations of tandem peptides and their derivatives. The backbone conformation is shown with a cartoon model. The most populated, second most populated, and third most populated backbone conformations are colored in green, cyan, and orange, respectively. These populated conformations were identified from 20 distinct and independent molecular dynamics simulations with an aggregated simulation time of 37.92 microseconds for each peptide (see Supplementary Table 1 for more information).

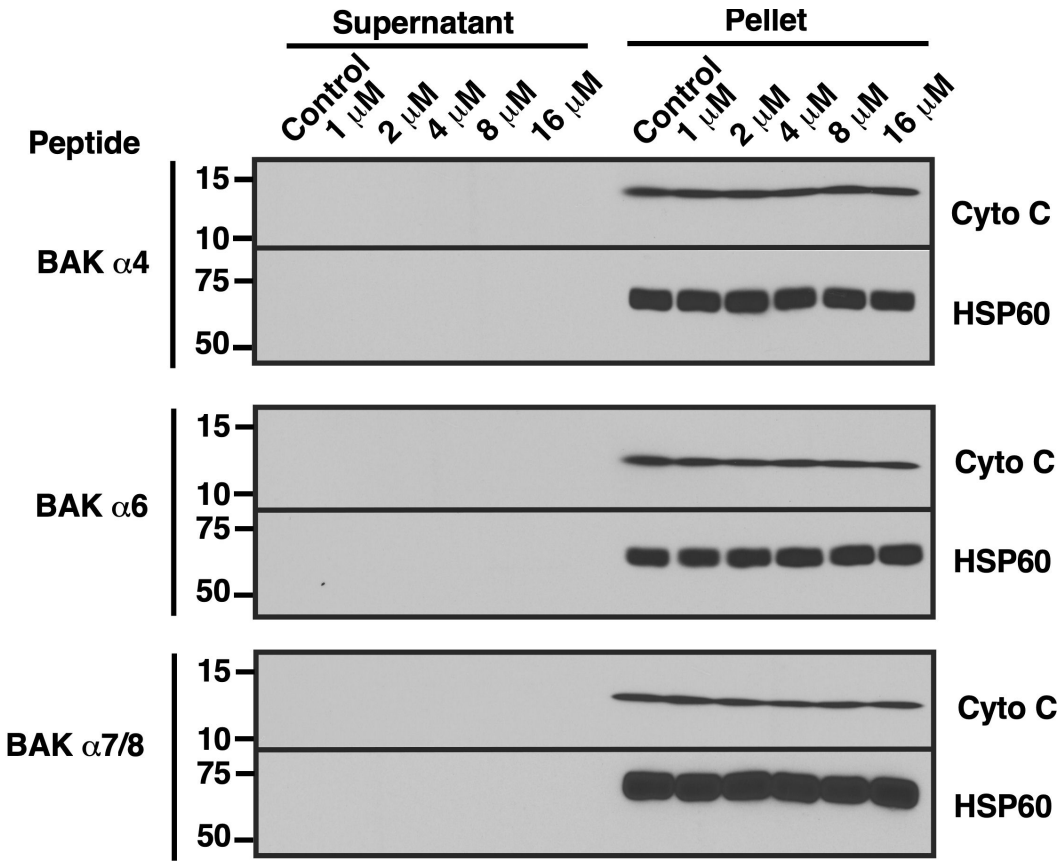

Figure S6 (related to Figure 4). Lack of mitochondrial permeabilization by α4, α6 or α7/8. After mitochondria from *Bax*$^{-/-}$*Bak*$^{-/-}$ MEFs were incubated with BAK peptides α4 (aa 105-123), α6 (aa 149-164), or α7/8 (aa 166-186) at 25 °C for 90 min, the supernatants and pellets were subjected to SDS-PAGE and immunoblotting.

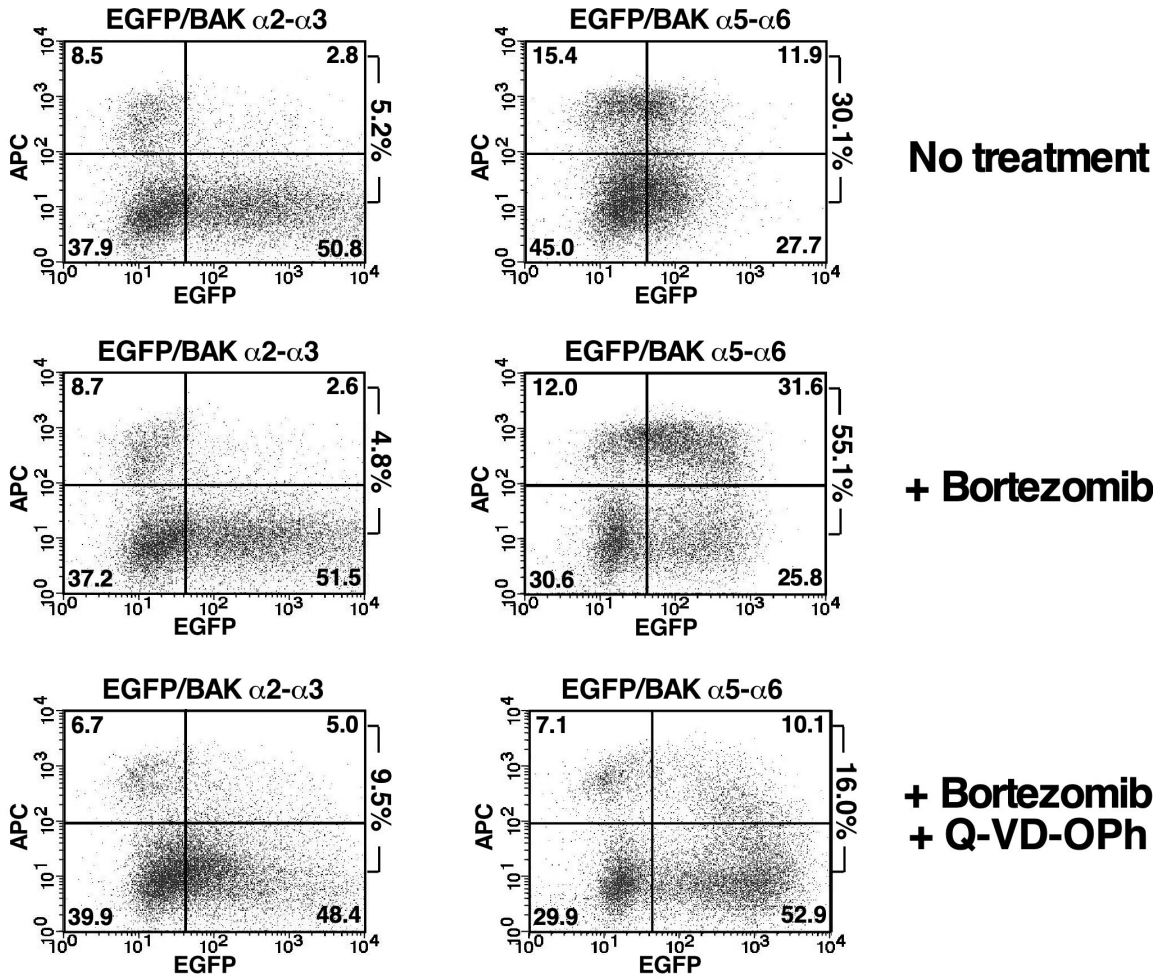

Figure S7 (related to Figure 4). Effect of bortezomib on EGFP-BAK domain expression and apoptosis in HCT116 *BAX*$^{-/-}$*BAK*$^{-/-}$ cells. HCT116 *BAX*$^{-/-}$*BAK*$^{-/-}$ cells were transfected with plasmids encoding EGFP-BAK α2-α3 (left) or EGFP-BAK α5-α6 (right) and incubated for 24 h in the presence of diluent (upper panel), 50 nM bortezomib (middle panel) or 50 nM bortezomib + 10 μM Q-VD-OPh (lower panel). At the end of the incubation, cells were stained with APC-annexin V and subjected to flow cytometry. Note the increased expression of EGFP/BAK α5-α6 (rightward shift of dots) in the presence of bortezomib. Numbers at the right of dot plots in this and subsequent figures are ratio of events in *upper right* panel to sum of *lower right* and *upper right*.

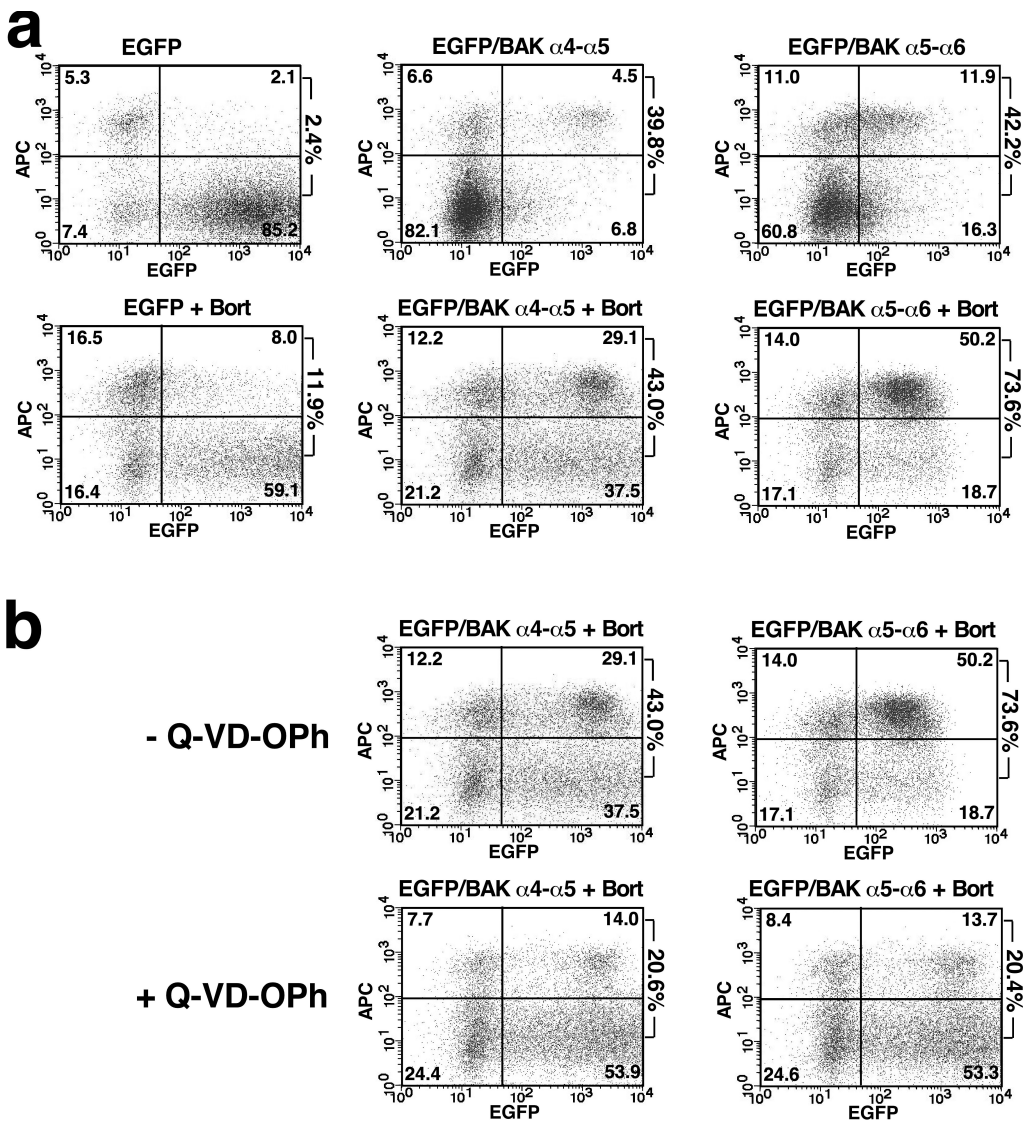

Figure S8 (related to Figure 4). Effect of bortezomib on EGFP-BAK domain expression and apoptosis in Jurkat *BAK*$^{-/-}$ cells. a Jurkat *BAK*$^{-/-}$ cells transfected with plasmids encoding EGFP (left), EGFP-BAK α4-α5 (middle) or EGFP-BAK α5-α6 (right) were incubated for 24 h in the presence of diluent (upper panel) or 15 nM bortezomib (lower panel). At the end of the incubation, cells were stained with APC-annexin V and subjected to flow cytometry. **b** Jurkat *BAK*$^{-/-}$ cells transfected with plasmids encoding the indicated EGFP-BAK domain fusion construct were incubated for 24 h in the presence of 15 nM bortezomib in the absence or presence of 10 μM Q-VD-OPh.

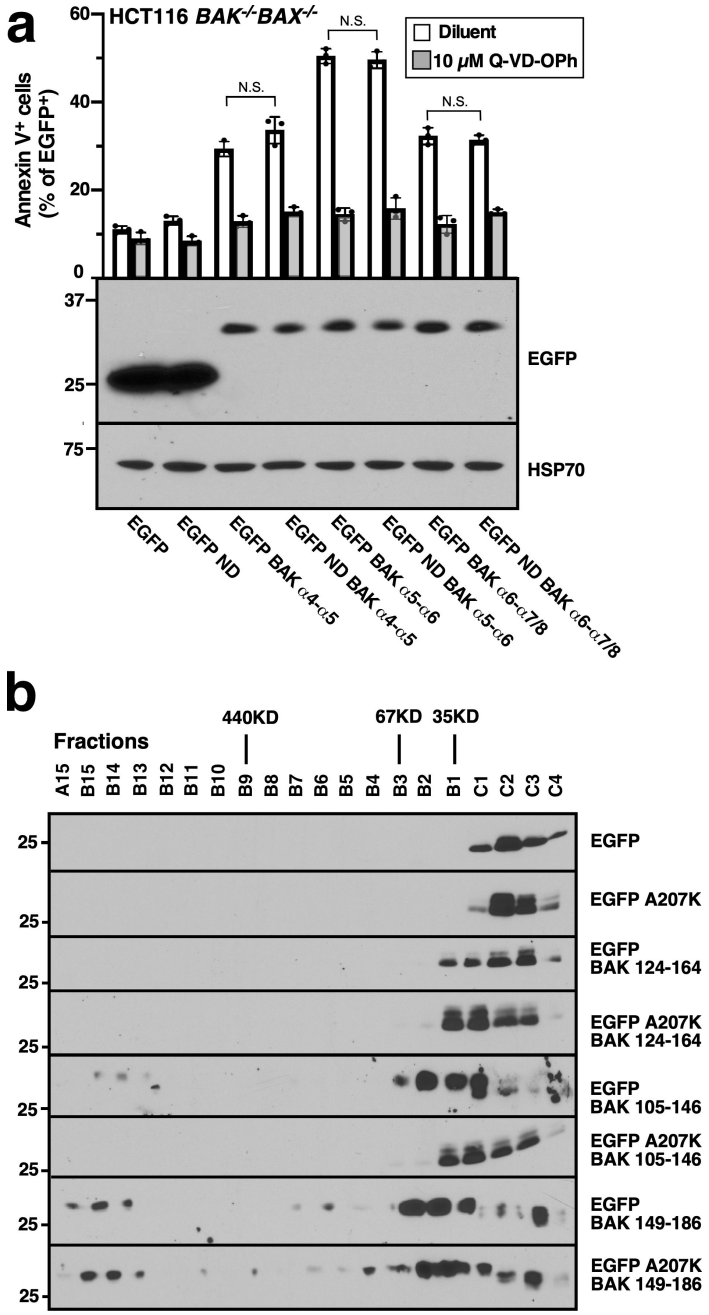

Figure S9 (related to Figure 4). BAK peptides permeabilize the MOM independent of EGFP oligomerization. a cDNAs encoding BAK peptides fused to the C-terminus of EGFP or nondimerizable (ND) EGFP A207K were transfected into *BAX*$^{-/-}$*BAK*$^{-/-}$ HCT116 cells. After incubation for 24 h in the presence 50 nM bortezomib ± 10 μM Q-VD-OPh, cells were stained with APC-Annexin V and analyzed for the percentage of EGFP^{+} cells that stained with Annexin V (bar graph). Immunoblots below graph show whole cell probed with anti-EGFP or, as a loading control, anti-HSP70. **b** Alternatively, after cells were incubated for 24 h in bortezomib ± Q-VD-OPh, lysates were prepared in CHAPS buffer and subjected to FPLC. Fractions were then analyzed by western blotting. Numbers at the top indicate the migration of molecular weight markers on the FPLC column. Error bars in a, mean ± SD of three independent experiments. N.S., indicated difference is not significant

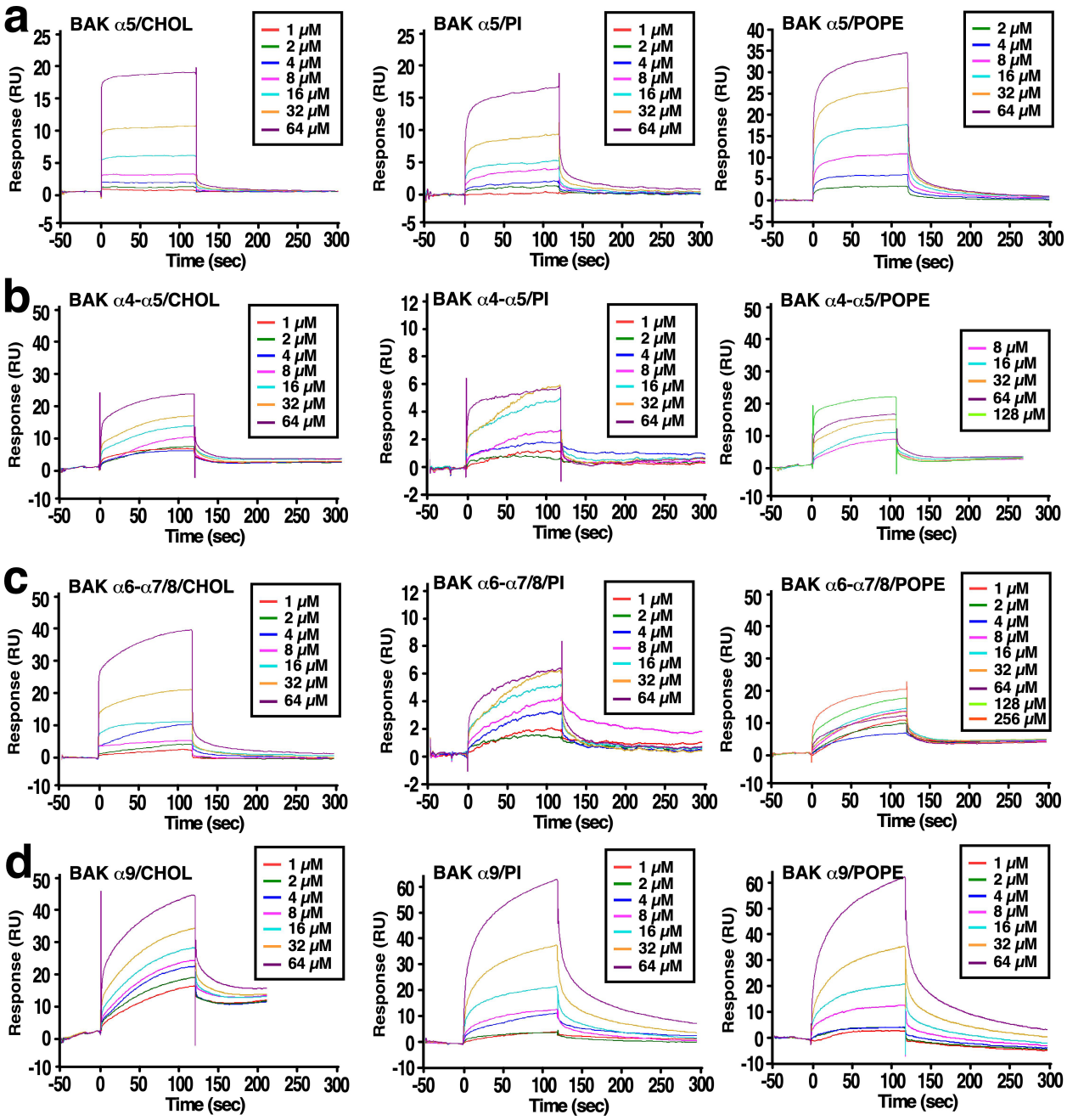

Figure S10 (related to Figure 5). Representative SPR sensograms. a-d Representative SPR sensograms of immobilized BAK α5 (a), α4-α5 (b), α6-α7/8 (c), or α9 (d) interacting with a series of cholesterol (CHOL, left), L-α-phosphatidyl-inositol (PI, middle) or POPE (right) concentrations.

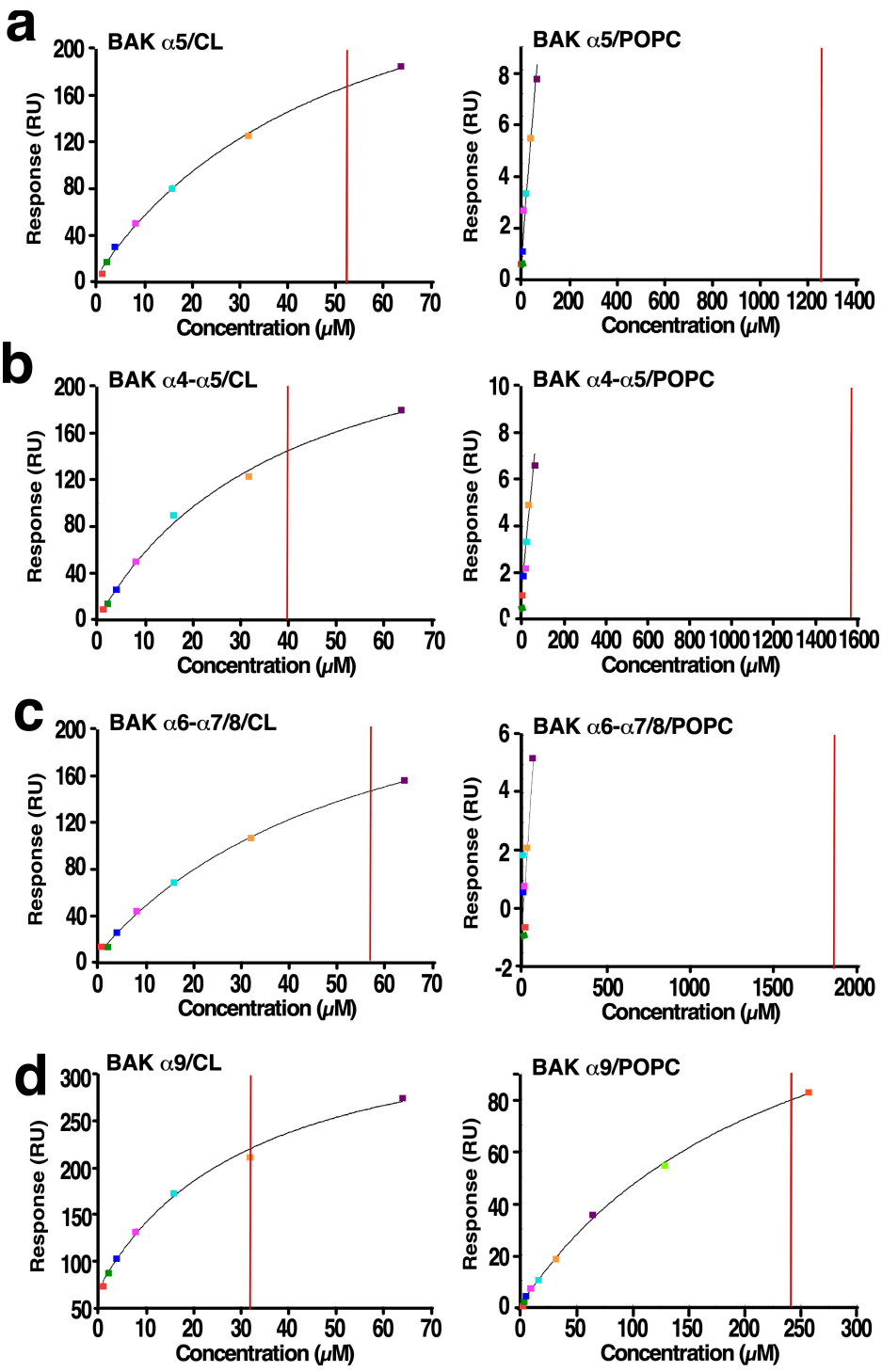

Figure S11 (related to Figure 5). Examples of calculation of K_Ds using steady state analysis and steady state analysis with constant R_{max}. a-d Responses (relative units, RU) of SPR chips with immobilized BAK α5 (a), α4-α5 (b), α6-α7/8 (c), or α9 (d) exposed to different concentrations of lipids were plotted as a function of lipid concentration. For CL (left panels), K_Ds were estimated as the concentration that RU reached half of R_{max} by steady state analysis. For POPC, KDs were estimated from R_{max} of POPC (calculated from the R_{max} of CL) using steady state analysis with constant R_{max}.

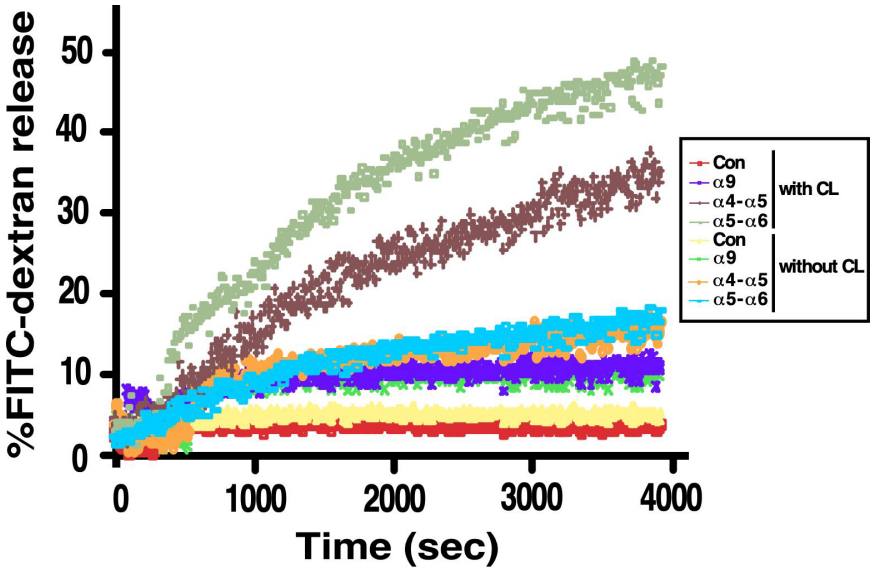

Figure S12 (Related to Figure 5). Impact of altered lipid composition on liposome permeabilization by BAK tandem peptides. After FITC-dextran-containing liposomes with different compositions [with CL (POPC:PE:PI:CL:CHOL = 41:22:9:20:8) or lacking CL (No CL, POPC:PE:PI:CL:CHOL = 61:22:9:0:8)] were mixed with the indicated BAK peptides (10 μM), the percentage of FITC-dextran released was measured as a function of time. This curve is from one of three independent experiments.

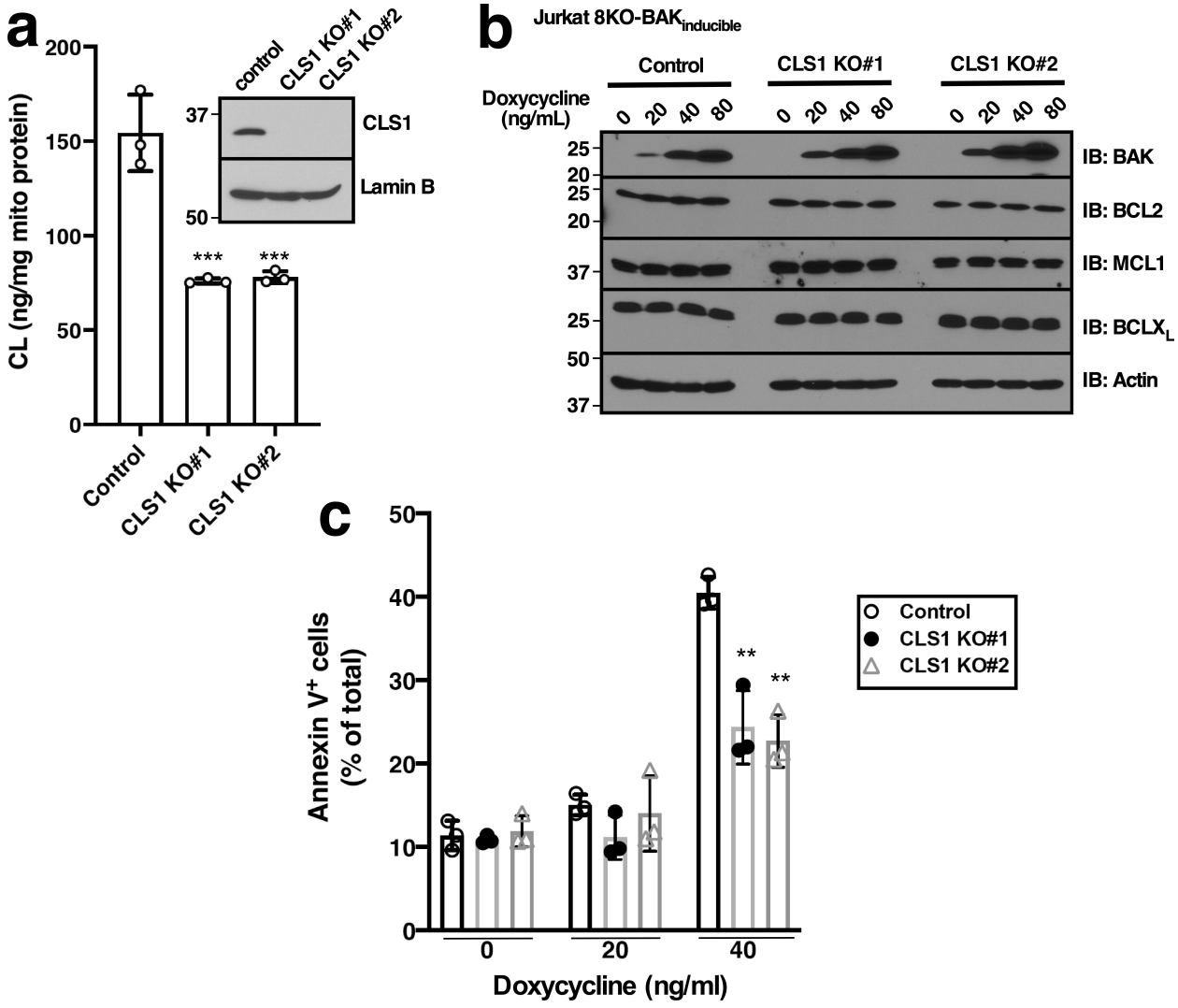

Figure S13 (related to Figure 5). Effect of *CLS1* gene interruption on BAK-induced apoptosis in Jurkat 8KO cells expressing doxycycline-inducible BAK. a Mitochondrial CL content in Jurkat 8KO/inducible BAK cells transduced with empty vector (pooled cells) or two different clones with targeted *CLS1* interruption. **Inset,** immunoblot of whole cell lysates prepared from the same populations used to isolate mitochondria. **b** After cells were treated for 16 h with the indicated concentration of doxycycline along with Q-VD-OPh to prevent caspase-medicated cell rupture, whole cell lysates were subjected to SDS-PAGE and blotting for the indicated BCL2 family member. **c** After cells were treated for 16 h with the indicated concentration of doxycycline in the absence of Q-VD-Ph, annexin V binding was assessed. Error bars in a and c, mean ± SD of three independent experiments. ** and ***, $p < 0.01$ and $p < 0.001$ relative to wildtype Jurkat cells (control).

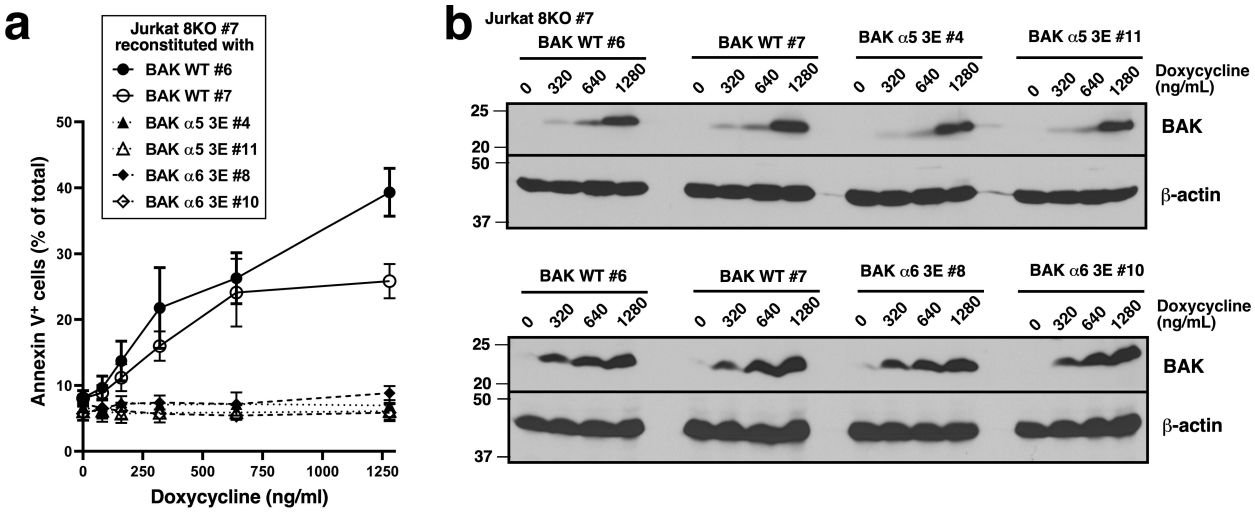

Figure S14 (Related to Figure 6). Mutations in α5 or α 6 of full-length BAK inhibit BAK-induced cell death. a Jurkat 8KO cells (lacking BAK, BAX, BID, BIM, PUMA, NOXA, BMF and HRK) were stably transfected with cDNA encoding BAK WT, BAK α5 3E (L131E/L132E/F134E) or BAK α6 3E (F157E/V159E/F161E) behind a doxycycline-inducible promoter. Two clones that expressed each construct in an inducible fashion were isolated by liminting dilution. After a 24-h treatment with the indicated concentrations of doxycycline, cells were stained with APC-Annexin V and subjected to flow microfluorimetry. **b** after aliquots of cells were incubated with indicated concentrations of doxycycline in the presence of Q-VD-OPh (to prevent caspase-mediated cell rupture) for 24 h, whole cell lysates were subjected to SDS-PAGE.

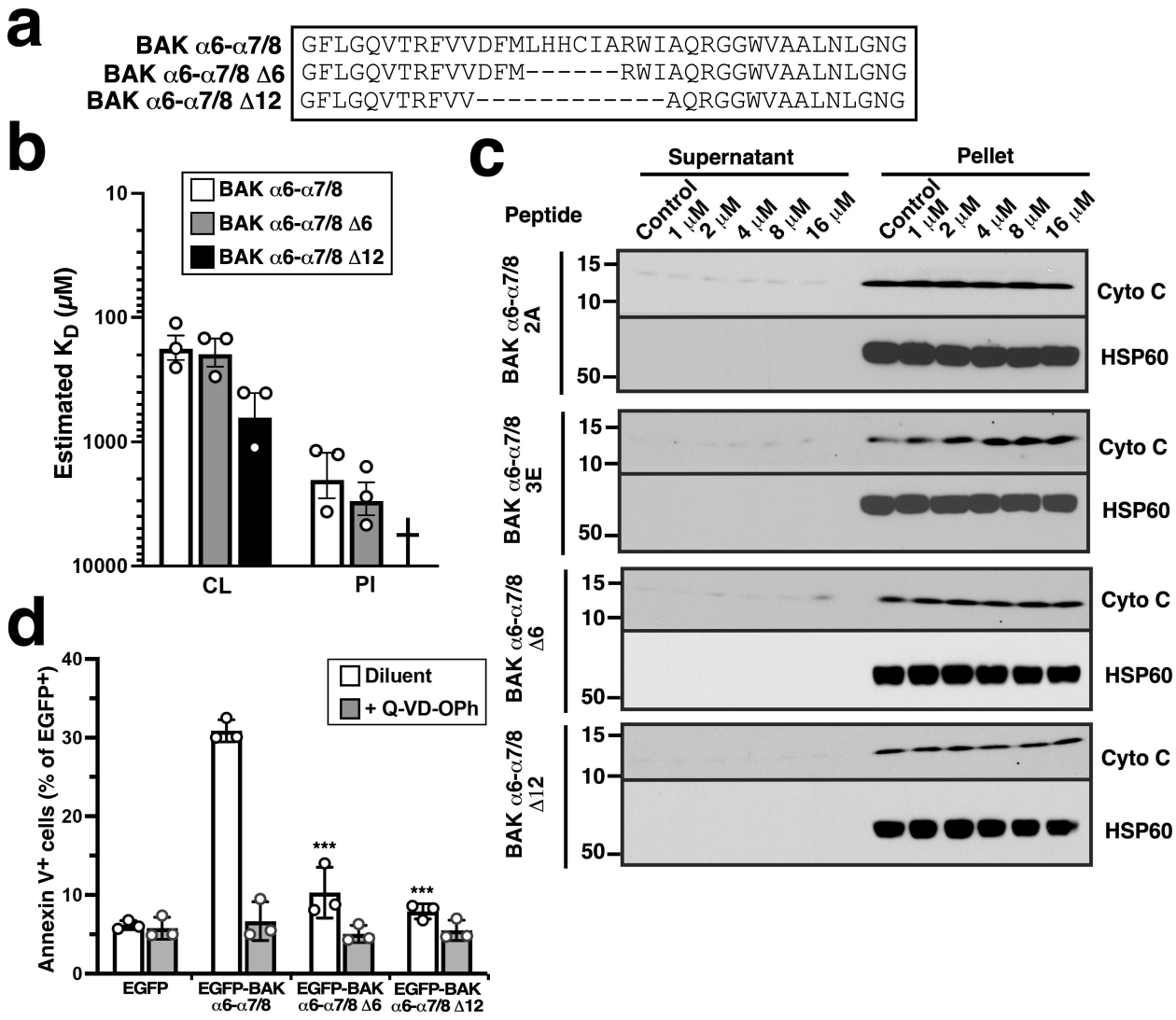

Figure S15 (Related to Figure 8). Effect of shortening of BAK α6-α7/8 on MOMP and cell killing. a Sequences of shortened BAK α6-α7/8 peptide mutants or EGFP-tagged peptide mutants used in panels b-e. **b** K_Ds of the indicated immobilized peptides interacting with CL or POPC as evaluated by SPR. **c** After mitochondria from *Bax*$^{-/-}$*Bak*$^{-/-}$ MEFs were incubated for 90 min at 25 °C with the shortened BAK α6-α7/8 peptides as indicated, supernatants and pellets were subjected to SDS-PAGE and immunoblotting. **d** cDNAs encoding EGFP-tagged BAK peptide variants were transfected into *BAX*$^{-/-}$*BAK*$^{-/-}$ HCT116 cells. After a 24-h incubation in the presence of bortezomib ± Q-VD-OPh, cells were stained with APC-Annexin V and subjected to flow microfluorimetry. Error bars in b and d, ± sd of 3 independent experiments. † in panel b, estimated K_D > 10 mM. *** in panel d, $p < 0.001$ compared to cells transfected with EGFP encoding unmodified α6-α7/8 at its C-terminus and incubated without Q-VD-OPh.

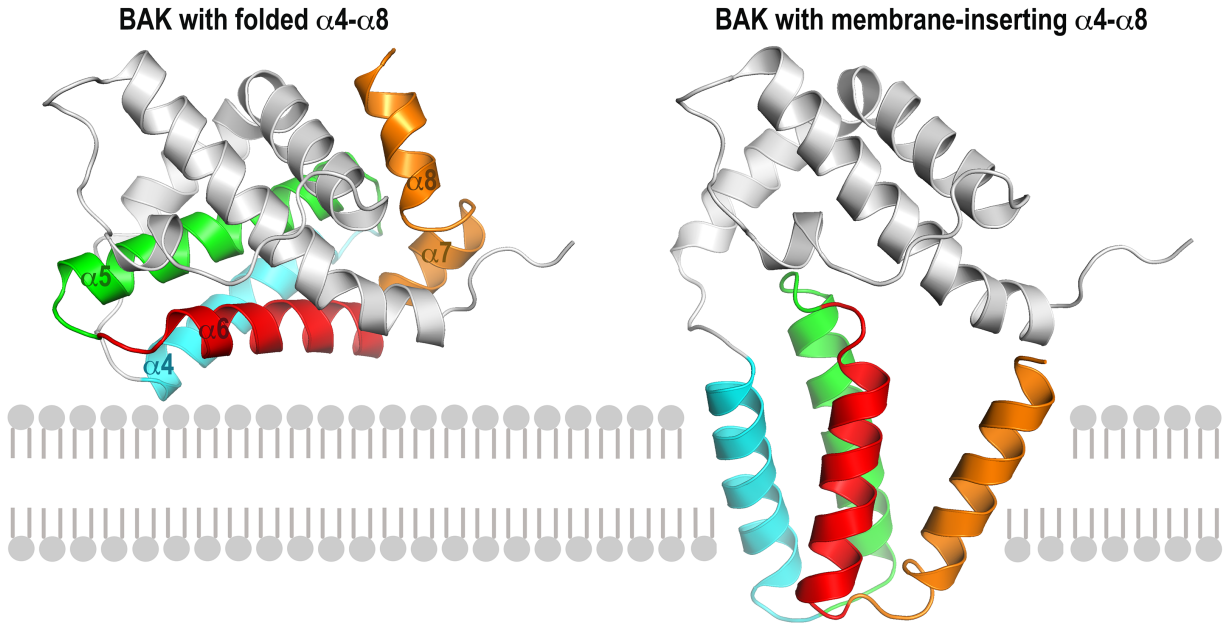

Figure S16 (Related to Figure 8). Alternative model of BAK α-helical domain interaction with MOM upon activation. See Discussion for additional details.